CHAPTER 4:

Characterization of biofilm components

4.1 Introduction:

Urinary tract infections (UTIs) account for 20% of death worldwide infecting serious human infections (Almalki and Varghese 2020). Of all nosocomial infections, Catheter-associated urinary tract infections (CAUTIs) represent 40% and are most prevalent among hospital-acquired infections (HAIs) (Nicolle et al. 2005; Jordan et al. 2015). These infections are persistent as they are caused by biofilm-forming bacteria. *P. aeruginosa* is found to be 3rd most common pathogen associated with hospital-acquired CAUTIs (Jarvis and Martone 1992b; Djordjevic et al. 2013). A study from the period 2012 to 2016 showed that 15% of bacterial isolates were represented from tertiary care hospitals (Kumari et al. 2019). *P. aeruginosa* is resistant to most antibiotics due to multiple modes of resistance mechanism and is capable of biofilm formation on various medical devices (Lister et al. 2009; Langendonk et al. 2021). Biofilm is defined as bacteria embedded in the self-produced matrix. *P. aeruginosa* biofilm is often difficult to eradicate as they are resistant to phagocytosis, and antibiotics as compared to planktonic counterparts and is persistent (Thi et al. 2020). Therefore, the key to treating biofilm-related infections and limiting the emergence of antibiotic resistance is the early diagnosis of biofilm producers. They are classified as strong, moderate, and weak biofilm producers to examine the quantitative variations between the biofilms produced by clinical isolates (Stepanović et al. 2004). Most widely used assay for quantifying biofilms is the crystal violet (CV) assay since it is simple and inexpensive (O'Toole 2010; Thibeaux et al. 2020). Although there are numerous ways to measure biofilms (Corte et al. 2019; Kragh et al. 2019); CV used here stains both total cells (live and dead cells) as well as the biofilm matrix. Therefore, it was used as a primary indicator to differentiate the biofilm producers. Recent studies have found that strong biofilm producers form thick biofilm having a high number of bacteria embedded in thick exopolymeric substances (Luther et al. 2018; Suriyanarayanan et al. 2018; Desai et al. 2019). Further, the exopolymeric substances of biofilm shield the enchased bacteria from harsh conditions, and dead bacteria provide necessary biomolecules for the remaining cells to survive (Webb et al. 2003; Ryder et al. 2007).

Composition of biofilm-matrix produced by typed strain (PAO1 and PA14) of *P. aeruginosa* is well characterized; where biofilm consisted of (i) polysaccharide (alginate, pel, and psl) (ii) proteinaceous components (type 4 pili, cdrA, ecotin, etc.) and, (iii) pyocyanin and (iv) extracellular DNA (eDNA) (Mulcahy et al. 2014; Thi et al. 2020). Previous studies on the murine model showed *P. aeruginosa* can form biofilm in absence of exopolysaccharides (Cole et al. 2014). Biofilm-associated matrix protein (i) CdrA (increases the stability of biofilm by

binding pel and psl exopolysaccharide) (ii) ecotin (binds to psl exopolysaccharide and increases the stability of biofilm) (Reichhardt et al. 2018; Tseng et al. 2018; Reichhardt et al. 2020). Biofilm formation of *P. aeruginosa* on various catheters has been documented (Xu et al. 2015; Tellis et al. 2017; Almalki and Varghese 2020) but a comparative analysis of biofilm matrix and biofilm-forming ability in UTIs isolates of *P. aeruginosa* are lacking.

The aim of the present study was to quantity the biofilm-forming abilities of *P. aeruginosa* isolates causing UTIs. Aso, biofilm formation on various catheters, adhesion ability, twitching motility, and arrangements of live-dead cells within the biofilm in strong and weak biofilm-producing isolates was studied.

4.2 Materials and Methods

4.2.1 Biofilm assay

According to Stepanovic et al 2004, biofilm quantification of UTI-causing *P aeruginosa* (n=22) and PAO1 (used as control) was done using crystal violet assay. In the 96-well microtiter plate, 20 µl of overnight grown culture (0.2 OD at 600 nm) and 230 µl LB (Luria Broth) were mixed and incubated at 37 °C for 24 hours in static conditions. The following day, planktonic cells were removed by rinsing biofilm twice with 0.85% saline; and later fixed with methanol for 15 minutes, and stained with crystal violet (CV) for 15 minutes. After washing, plates were air-dried for 15 minutes. The stained biofilm was treated with 33% glacial acetic acid which dissolved bound CV from biofilm. Further, Biofilm was quantified spectrophotometrically at 570 nm. Isolates were classified based on their cut-off OD (ODc) values as strong, moderate, or weak biofilm producers (Stepanović et al. 2004). The cut-off OD value was determined as three standard deviations above the mean OD of the negative control. Isolates were classified as no biofilm producer ($OD \leq ODc$), weak biofilm producers ($ODc < OD < 2 \times ODc$), moderate biofilm producers ($2 \times ODc < OD < 4 \times ODc$), and strong biofilm producers ($4 \times ODc < OD$). All experiments were performed in triplicates.

4.2.2 Growth curve

The following isolates of each category strong (ST-20, TP-25, TP-35, and TP-48) and weak (ST-22, TP-8, TP-10, and TP-11) biofilm producers were selected for further study. The growth curve was studied using 100 µl of bacterial culture (OD at 600 nm ~ 0.05) grown in LB and inoculated in a sterile 96-well flat-bottomed plate and incubated at 37 °C for 12 hours. The reading was continuously measured at 15 minutes intervals for 12 hours using HT microtiter plate reader (Biotek Instruments, Winooski, VT, USA). The growth curve was plotted and the growth rate was determined for each strain.

4.2.3 In vitro biofilm quantification on catheters

Above mentioned isolates of strong and weak biofilm producers were used for biofilm quantification on catheters (silicone-coated latex and latex catheters). Briefly, a 1 cm long piece of the catheter was cut vertically into 2 pieces, sterilized in methanol, and air-dried. In 24 well plates, catheters were kept in a 2 ml system with 1:10 diluted (0.2 OD at 600 nm) culture in LB and incubated at 37 °C for 24 hours. Biofilm formation on catheters was quantified using a modified CV assay for which the catheter piece was kept in a new plate, fixed with methanol for 15 minutes, and stained with 0.1% CV. After being washed twice with 0.85% NaCl, the plate was air-dried, bound CV was dissolved in 33% glacial acetic acid, and measured

spectrophotometrically at 570 nm. Biofilm formed in presence of Natural Urine (NU) (obtained from a healthy volunteer, filter sterilized through a 0.2 µm filter, and stored at -20 °C for further use) and Artificial Urine (AU) (composition:2.43% urea, 1% NaCl, 0.6% KCl, 0.64% Na_2HPO4, 0.05 mg/mL albumin, pH 7) were quantified using the same assay. For negative control: LB, NU, and AU having catheters without bacterial culture were used respectively. The experiment was performed in triplicates for each strain.

4.2.4 Field Emission Gun Scanning Electron Microscope (FEG-SEM)

The FEG-SEM was performed for strong (TP-25) and weak (TP-8) biofilm producer's biofilm grown on silicone-coated latex catheters, as mentioned in the above protocol. Biofilm was rinsed with sterile Phosphate Buffer Saline (PBS) after incubation, fixed with 2% glutaraldehyde in PBS at 4 °C overnight, then sequentially dehydrated with 30, 50, 70, 90, and 100% ethanol in order.

4.2.5 Light microscopy

The adhesion ability of strong (n=4) and weak (n=4) biofilm producers was studied on the coverslip using a light microscope. In the 6 well plates (having glass coverslip), 5 ml of 1:10 diluted bacterial culture (0.2 OD at 600 nm) in LB was inoculated and incubated at 37 °C for 4 hours in static conditions. Following incubation, the unadhered cells were washed off with 0.85% NaCl, Gram staining was performed, and observed under 100X magnification (BX 51 Olympus microscope, Japan). The adhered cells on the coverslip were counted using Fiji software.

4.2.6 Twitching motility

To determine twitching motility for previously mentioned strong (n=4) and weak (n=4) biofilm-producers, 1% Luria agar (LA) plates were stabbed and incubated for 24 hours at 37 °C, followed by measurement of twitching zones (Darzins 1993). By Phase-contrast time-lapse microscopy, twitching ability was observed under a 100X oil immersion microscope. Briefly, 1 µl (0.2 OD at 600 nm) of bacterial culture was spotted on a 1% LA pad (LA was air dried) and observed for 4 hours and 24 hours. The experiment was performed in triplicates.

4.2.7 Gene Expression analysis

4.2.7.1 RNA isolation

Type 4 pili and biofilm matrix protein *cdrA* gene were studied from 4 hours and 24 hours biofilms from strong and weak biofilm producers. For RNA isolation, biofilm was washed and resuspended in 1 ml of 0.85% NaCl to remove any residual media. Further RNA isolation was

carried out through a Nucleospin RNA kit (Macherey Nagel, Hoerdt, France) where cell pellet obtained after centrifugation was resuspended in 100 µl TE buffer containing 1 mg/mL lysozyme by vigorous vortexing and later incubated at room temperature (RT) for 10 minutes. After incubation, 350 µl of RA1 buffer and 3.5 µl of β-mercaptoethanol (to eliminate ribonuclease (RNases) released during cell lysis) were added to the suspension and vortexed for 30 seconds. To reduce the viscosity and obtain clear lysate, suspension was filtered through NucleoSpin® Filter (violet ring): (make sure to place the NucleoSpin® Filter in a Collection Tube of 2 mL), and centrifuged for 1 min at 11,000 x g. Further, the NucleoSpin® filter was discarded, then to the homogenized lysate 350 µl of 70% ethanol was added and was gently mixed by pipetting. One NucleoSpin® RNA Column (with a light blue ring) was taken and place it in a collection tube. Lysate was gently mixed by pipetting times and lysate was loaded into the column (having a blue color filter ring) and centrifuge for 30 seconds at 11,000 x g. To the same column, 350 µl of Membrane Desalting Buffer (MDB) was added to dry the membrane and centrifuged at 11,000 g for 1 minute. DNase treatment was given by preparing the reaction mixture in a sterile 1.5 ml microcentrifuge tube (the tube was DEPC treated and autoclaved). For each RNA isolation, 10 µl of reconstituted rDNase was added to 90 µl of Reaction Buffer and mixed by flicking the tube. Onto the center of the silica membrane, 95 µl of DNase reaction mixture was added directly, which was then incubated at RT for 15 minutes. After incubation, to NucleoSpin® RNA column, 200 µl of buffer RAW2 was added and centrifuged at 11,000 g for 30 seconds. Lysate was discarded from the collection tube. 600 µl of RA3 buffer was added to the NucleoSpin® RNA Column and centrifuged at 11,000 g for 30 seconds (this step was repeated twice). Flowthrough was discarded and column back was placed onto the collection tube. Later, 250 µl RA3 buffer was added to the NucleoSpin® RNA Column and centrifuged at 11,000 g for 2 minutes to dry the membrane completely. For the collection of RNA, the column was placed into new nuclease-free collection tube. RNA was eluted in 20 µl of RNase-free water and centrifuged at 11,000 x g for 1 minute. RNA was run on a 2% gel, to determine its integrity quantification was carried out using Nanodrop (Thermo Fisher Scientific, Waltham, Massachusetts, USA).

4.2.7.2 cDNA synthesis

From total RNA cDNA synthesis was done using PrimeScript™ cDNA Synthesis Kit (Takara Bio Inc., Shiga, Japan) as per the manufacturer's instruction. Reaction system-1 used is depicted in Table 4.1. Reaction system-1 was incubated at 65 °C for 5 minutes and placed on ice for 5 minutes. Reaction system-II was then set up as shown in Table 4.2. The reaction

system-2 was then incubated under the following conditions: 30 °C for 10 minutes; 50 °C for 1 hour and 70 °C for 5 minutes. The reaction mixture was then stored at -20 °C.

Table 4.1: Reaction system-1 for cDNA synthesis

Reaction Component	Volume
Rand-6-mers	2 µl
dNTP mix	1 µl
Template RNA	500 ng
RNase free water	X µl
Total system	10 µl

Table 4.2: Reaction system-2 for cDNA synthesis

Reaction Component	Volume
Reaction system I	10 µl
5X Prime Script Buffer	4 µl
RNase inhibitor	0.5 µl
Reverse Transcriptase	1 µl
RNase free water	4.5 µl
Total system	20 µl

4.2.7.3 Primer Designing for qRT-PCR

The primers for gene *pilA* (For type 4 pili expression) and *cdrA* (for extracellular protein) were designed using the SnapGene software. Table 4.3 shows the list of primer sequences used in qRT-PCR.

Table 4.3: Primer used for qRT-PCR for type 4 pili expression

Primers	Sequences (5'-3')
pilA_F	CCAGCAATTCCACGCGACAG
pilA_R	CGAACTGATGATCGTGGTTGCG
cdrA_F	CCCAGTTCAACCCCAACGAG
cdrA_R	GCTGGTTGAAGCGCACCG
rpoD_F	GGGCGAAGAAGGAAATGGTC
rpoD_R	CAGGTGGCGTAGGTGGAGAA

4.2.7.4 Gene expression studies using qRT-PCR

Gene expression of *pilA* and *cdrA* genes was studied mong strong and weak biofilm producers using SYBR Green (Takara Bio Inc., Shiga, Japan). The *rpoD* gene was used as a housekeeping gene. Internal gene normalization was done using *rpoD* gene and fold change was calculated as per the $2^{-\Delta\Delta Ct}$ method (Guyard-Nicodème et al. 2008). The gene was considered to be overexpressed if there was 2-fold change expression compared to weak biofilm producers. . Relative quantification of genes was carried out using three biological triplicates. The above Table 4.3 shows primer sequence used for qRT-PCR. Reaction system for qRT-PCR is shown in Table 4.4, and the qRT-PCR cycle is shown in Table 4.5.

Table 4.4: Reaction system used for qRT-PCR

Reaction Component	Volume
SYBR Green master mix	5 µl
AMQ water	2 µl
Forward Primer	1 µl
Reverse Primer	1 µl
cDNA Template	1 µl
Total System	10 µl

Table 4.5: Condition used for qRT-PCR

Step	Temperature ºC	Time
Initial denaturation	95	3 minutes
Denaturation	94	30 seconds
Annealing	57	30 seconds
Primer Extension	72	30 seconds
Repeat cycle 35 X		
Final extension	72	5 minutes
Melt curve	65 to 95 increments 0.5	0.05 seconds

4.2.8 Confocal Laser Scanning Microscopy (CLSM)

The 24 hours old biofilm formed by strong and weak biofilm producers was visualized using Carl Zeiss CLSM 780 and 710 microscopes. Briefly, biofilm was grown on a glass coverslip in 6 well plates in LB medium with 1:10 diluted (0.2 OD at 600nm) overnight grown culture The following day, biofilm was rinsed with 0.85% NaCl to remove planktonic cells. The staining of biofilm attached to the coverslip was done with Syto9 (stains live cells in green color) and PI (stains dead cells in red color) dye from LIVE/DEAD® *Bac*Light™ Bacterial Viability Kit for 10 min. Further, biofilm was rinsed to remove excess stains. The 3D structure of biofilm was captured by CLSM using Z-stack. Fiji software was used to measure live and dead cells.

4.2.9 Quantification of biofilm matrix components

According to Wu and Xi 2009, eDNA and extracellular protein were extracted with few modifications and was normalized with OD at 600nm. The 2 ml of 1:10 diluted (0.2 at OD 600nm) culture in LB medium was inoculated in 24 well plates and incubated at 37 °C for 24 hours. The following day, the biofilm was rinsed with 0.85% NaCl; resuspended in 1 ml of 0.85% NaCl and homogenized by vortexing for 30 seconds. The bacterial cells were removed by passing them through a 0.22 µm filter (Wu and Xi 2009). Filtered solution was used for eDNA and extracellular protein quantification.

4.2.9.1 eDNA quantification:

From 500 µl filtered solutions (above), eDNA was extracted using the phenol-chloroform method (Wu and Xi 2009) and quantified by measuring absorbance at 260 nm using nanodrop (Thermo Fisher Scientific, Waltham, MA, USA). The eDNA concentration was normalized with OD at 600 nm.

4.2.9.2 Extracellular protein quantification:

The 100 µl of the filtered solution was added to Bradford reagent and incubated for 10 min. Absorbance was measured at 595 nm and extracellular protein was normalized with OD 600 nm. The experiment was performed in triplicates.

4.2.9.3 Pel polysaccharide quantification

The Pel-dependent EPS was quantified using the amount of Congo-red binding assay (Madsen et al. 2015). Overnight grown culture was 1:10 diluted (0.2 OD at 600 nm) and inoculated in 2 ml LB kept at 37 °C for 24 hours. The next day, bacterial content, as well as EPS, was centrifuged to obtain pellet which was resuspended in 1 ml LB (containing 40 mg/ml Congo red), and incubated for 2 hours at 37 °C at 250 rpm. After incubation, EPS was collected by centrifugation, the supernatants were collected from each suspension, and absorbance was measured at 490 nm. The LB containing 40 mg/mL Congo-red was used as a blank. The experiment was performed in triplicates for each strain of strong and weak.

4.2.9.4 Alginate polysaccharide quantification

Alginate extraction and quantification were done using Jones et al., 2013 and Cesaretti et al. 2003. 24 hours bacterial colony was scraped out, resuspended in 0.85% NaCl, and collected by centrifugation (12,000 × *g* for 30 minutes). The supernatant was treated with 2% Cetyl Pyridiniuum Chloride before centrifugation to extract alginate. Further, the pellet was resuspended in 1 ml of 1M NaCl, then precipitated with cold isopropanol, and resuspended in 0.85% NaCl. With 96-well format modifications (Knutson and Jeanes 1968), alginate quantification was determined by carbazole assay (Cesaretti et al. 2003). The reaction was carried out using 50 µl of resuspended alginate treated with a 200 µl borate-sulfuric acid reagent (10 mM H_3BO_3 in concentrated H_2SO_4) at 100 °C for 15 minutes then 50 µl of carbazole reagent (0.1%) was added to above mixture and heated to 100 °C for 10 minutes. The absorbance at 550 nm (Multiskan Go, Thermo Fisher Scientific, Waltham, MA, USA) was used to quantify alginate. To determine the concentration of alginate, standard seaweed alginate was used. The experiment was performed three times for each strong and weak biofilm producers.

4.2.9.5 Pyocyanin Quantification

According to Essar et al.1990, pyocyanin production by strong (n=4) and weak (n=4) biofilm producers was measured. Briefly, 1:10 diluted (0.2 OD at 600 nm) overnight grown culture was inoculated in 2 ml LB medium and incubated at shaking at 37 °C for 24 hours. The following

day, the culture was centrifuged, and a supernatant was used to extract pyocyanin with 3 ml chloroform and re-extracted with 0.1N HCl. The absorbance was measured at 520 nm and multiplied it by 17.02 to obtain concentration as µg of pyocyanin per ml of supernatant (Essar et al. 1990). The 0.2M HCl was used as blank. The experiment was performed in three biological replicates for each strain.

4.2.9.6 Rhamnolipid quantification

1:10 diluted (0.2 OD culture at 600 nm) overnight grown culture was inoculated in LB medium and kept at 37 °C for 24 hours. The next day, 4 ml of the supernatant was taken and pH was adjusted to 2.3 ± 0.2 using 1N HCl. Rhamnolipid was extracted with 5 volumes of chloroform, to chloroform extract 200 µl of 1 g/L methylene blue solution (pH of methylene blue was adjusted to 8.6 ± 0.2 by adding 50mM Borax buffer), and 4.9 ml distilled water was added. The sample was mixed and kept at RT for 15 minutes. The chloroform phase was measured at 638 nm and normalized with the A_{600nm} (Pinzon and Ju 2009). Only chloroform was used as a blank. The experiment was performed in triplicates for each strain.

4.2.10 Enzymatic digestion of biofilm

The biofilm was grown in the 96-well microtiter plate for each strong (n=4) and weak (n=4) biofilm producer as per the biofilm assay and kept at 37 °C for 24 hours. The following day, planktonic cells were removed and treated with 100 µg/ml of DNase, RNase, and Proteinase K each in separate wells, and further incubated at 37 °C for 24 hours (Tetz et al. 2009). After 24 hours of incubation, the biofilm was rinsed with 0.85% NaCl and the biofilm formed was quantified using CV assay. The LB medium with culture was used as a control. Only LB medium was used as a blank. The experiment was performed in triplicates for each strain.

4.2.11 Addition of eDNA and extracellular protein in biofilm

An additional assay was performed to validate the role of eDNA and extracellular protein in the biofilm (Harmsen et al. 2010). Biofilm was formed as described above, with the addition of *P. aeruginosa* extracted eDNA (100 ng/ml), genomic DNA (100 ng/ml), and extracellular protein (3µg/ml) and incubated at 37 °C for 24 hours (Harmsen et al. 2010). The following day, planktonic cells were washed off and the CV assay was done as described above. LB with bacterial culture was used as control and only LB served as blank. The experiment was performed in three biological replicates for each strain.

4.2.12 Statistical analysis

The experiment was performed in biological triplicates for each strain. Corresponding data represents mean ± standard deviation (SD). The student's t-test and two-way ANOVA were performed using GraphPad Prism 9 software (GraphPad, San Diego, USA). Differences were statistically significant at $P<0.05$.

4.3 Results

4.3.1 Biofilm categorization of UTI isolates of *P. aeruginosa*

Biofilm-forming ability of UTI-causing *P. aeruginosa* (n=22) was studied in the 96-well plate using CV assay and further categorize into strong, moderate, and weak biofilm producers based on cut-off OD value. Majority of the isolates were identified as strong (n=16), moderate (n=2), and weak (n=4) biofilm producers (Figure 4.1a). For further study strong (ST-20, TP-25, TP-35and TP-48) and weak (ST-22, TP-8, TP-10, TP-11) biofilm producers were randomly selected. The average growth rate of strong (n=4) and weak (n=4) biofilm producers was 0.24 ± 0.021 per hour (Figure 4.1b). One of the isolates from each strong and weak biofilm producer appeared to be a slow grower, however, no statistical significance was observed (Figure 4.1b).

4.3.2 Biofilm quantification on catheters

In vitro biofilm quantification of strong (ST-20, TP-25, TP-35and TP-48) and weak (ST-22, TP-8, TP-10, TP-11) biofilm producers were studied on different catheters: silicone-coated latex and silicone catheters. strong and weak biofilm producers formed maximum amount of biofilm on LB followed by NU and AU on both catheters (Figure 4.2a and b). Regardless of the medium used there was no significant difference in biofilm formation by strong producers on silicone-coated latex in comparison with silicone catheters (Figure 4.2c). However, in presence of LB highest biofilm formation was observed on silicone-coated latex catheters by weak biofilm producers compared to silicone catheters (Figure 4.2 c) and no negligible difference was observed between NU and AU (Figure 4.2c). Furthermore, strong biofilm producers formed highest biofilm on silicone catheters in LB when compared to weak biofilm producers (Figure 4.2d).

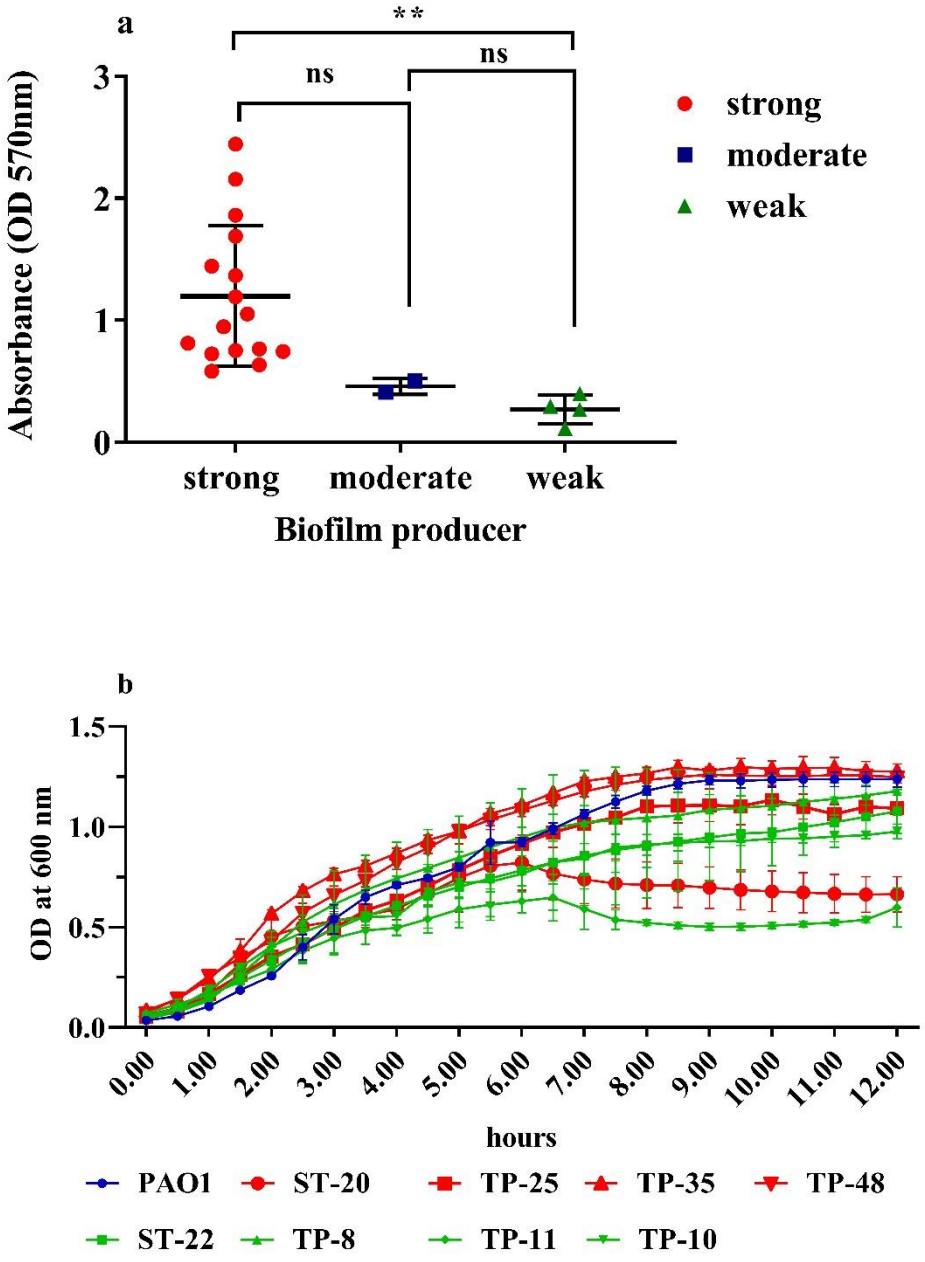

Figure 4.1: Biofilm quantification. Biofilm quantification of UTIs causing P. aeruginosa (n=22) was done using crystal violet assay in the 96-well plate and categorized into strong, moderate, and weak biofilm producers. (b) Growth curve of strong (ST-20, TP-25, TP- 35, TP-48) and weak (ST-22, TP-8, TP- 10, TP-11) biofilm producers. The experiment was performed in triplicates. The statistical significance for biofilm quantification represents an unpaired t-test using GraphPad Prism 9, where the p value represents ** $P < 0.005$.

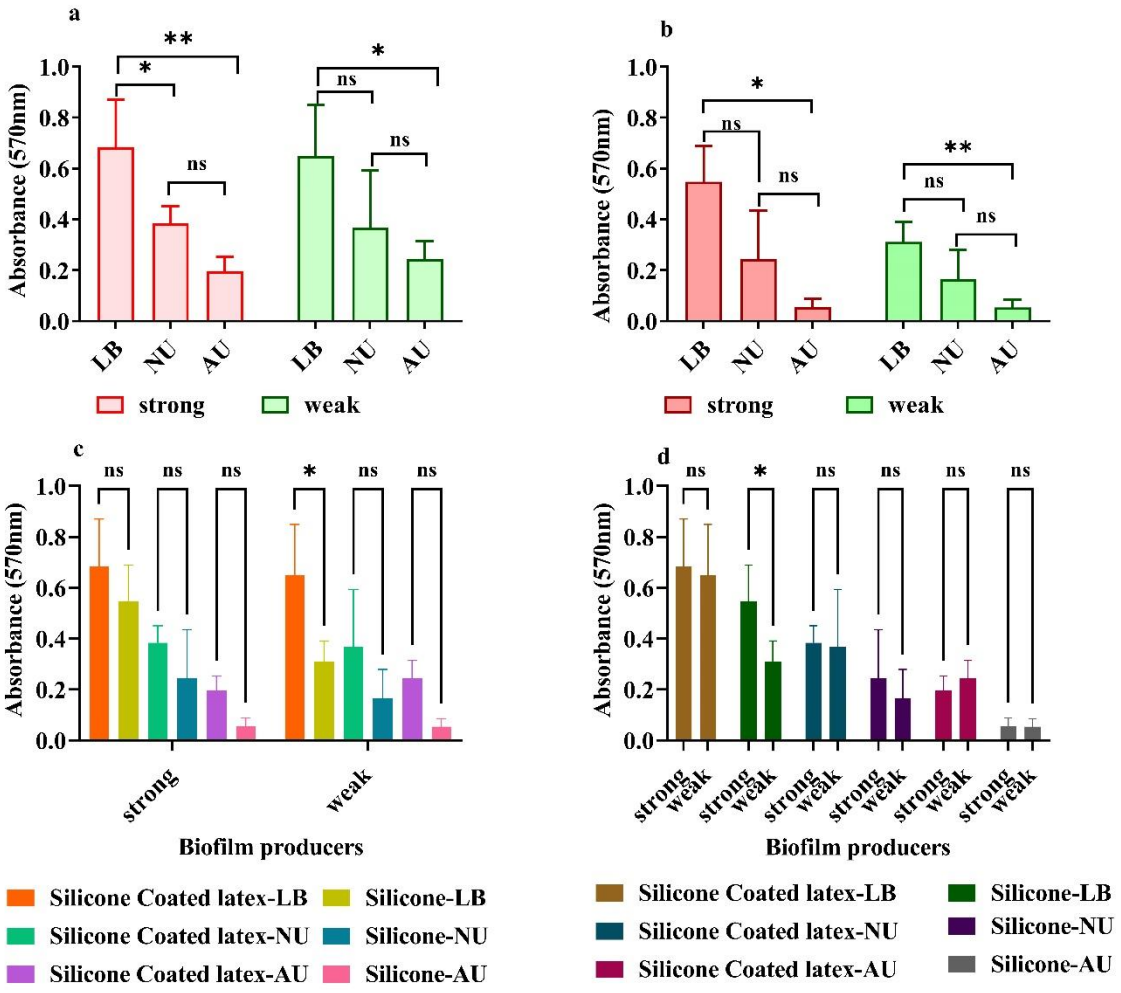

Figure 4.2: Biofilm quantification on catheters. Biofilm quantification was done in a 24-well plate using crystal violet assay on (a) silicone-coated latex and (b) silicone catheters in presence of LB, NU, and AU using crystal violet assay. (c and d) Statistical comparison of strong and weak biofilm producers. Experiment was performed in three triplicates for each strain. Statistical analysis was performed using Two-way ANOVA, where the values were significant ns $P > 0.05$, * $P < 0.05$, ** $P < 0.005$, *** $P < 0.0005$.

4.3.3 FEG-SEM of biofilm on catheters

Biofilm formed on silicone-coated latex catheters by strong (TP-25) and weak (TP-8) biofilm producers was studied through FEG-SEM. At 3000X magnification, biofilm formed on silicone-coated latex catheter by strong (TP-25) showed thick biofilm, also cells were not visible due to thick biofilm. (Figure 4.3a upper left panel). Whereas, thin layer of bacteria adhered to catheter in weak biofilm producers, and less EPS was observed (Figure 4.3b lower left panel). Further magnification at 6000X, rod-shaped cells encased within EPS matrix were observed in strong biofilm producers (Figure 4.3a; upper middle panel); on the other hand, cells adhered to each other, bound to catheter, and EPS matrix was barely visible in weak biofilm producers (Figure 4.3b; lower middle panel). Increased magnification to 12000X further confirms that cells are encased within EPS matrix having a dense mass with the irregular surface of strong biofilm producers (Figure 4.3a upper right panel). While cells were aggregated and microcolony formation was barely visible in weak biofilm producers (Figure 4.3b; lower right panel).

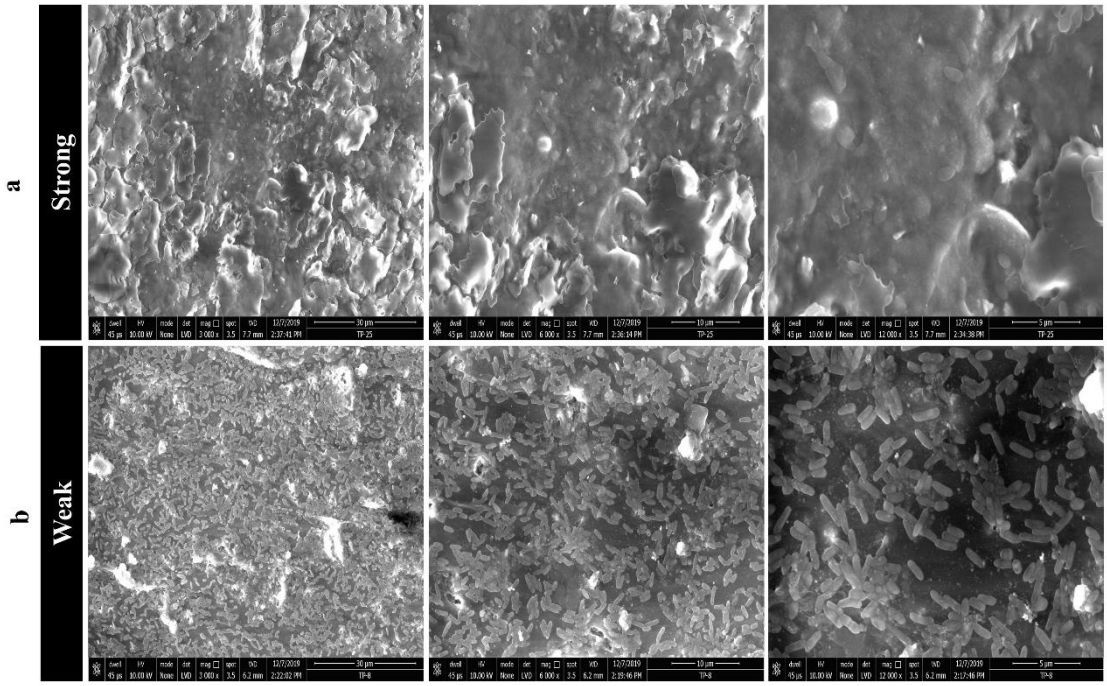

Figure 4.3: FEG-SEM of biofilm. Biofilm was formed on catheters for 24 hours in LB and then subjected for FEG-SEM. The representative images of biofilm formed by (a) strong and (b) weak biofilm producers on silicone-coated latex catheter at 3000X (left panel), 6000X (middle panel) and 12000X (right panel) magnification.

4.3.4 Adhesion assay

The ability of strong and weak biofilm producers to adhere to coverslip was studied after 4 hours of incubation in an LB medium. Strong biofilm producers had a higher number of cells attached to the coverslip as shown in light microscopy images than weak biofilm producers (Figure 4.4a). Strong (n=727 ± 100) biofilm producers had a considerably higher number of cells attached to the coverslip than weak (n=127 ± 29) biofilm producers (Figure 4.4b).

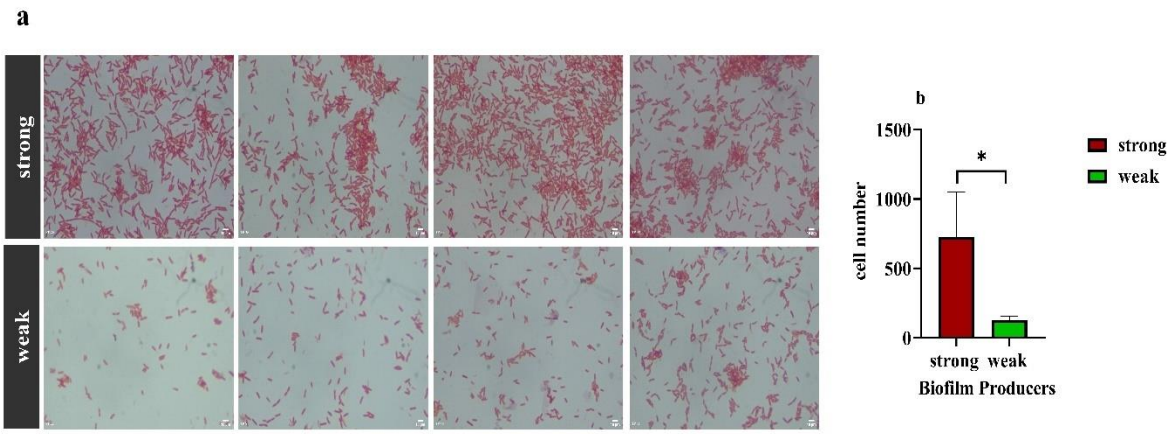

Figure 4.4: Cell adhesion. (a) Representative images of cell adhesion were studied on coverslip after 4 hours of adhesion in LB medium on strong (ST-20, TP-25, TP- 35, TP-48) and weak (ST-22, TP-8, TP- 10, TP-11) biofilm producers. (b) Cell count of adhesion assay of strong (n=4) and weak (n=4) biofilm producers. Data represent three biological triplicates for each strain. The statistically significant represents Student's t-test was * $P < 0.5$.

4.3.5 Twitching motility

For surface attachment through the irreversible mechanism and initial stage of microcolony formation twitching motility mediated by type 4 pili (T4P) is required. Twitching motility of strong and weak biofilm producers was then studied. Figure 4.5a shows the representative image of twitching motility on 1% LA plates of PA01, strong (TP-25), and weak (TP-8) biofilm producers. The twitching zone of strong (1.1 ± 0.40 mm) and weak (0.6 ± 0.21 mm) biofilm producers showed a significant difference (Figure 4.5c). Further, the twitching motility of strong and weak biofilm producers was observed under phase-contrast time-lapse microscopy. Through phase-contrast time-lapse microscopy, it was observed that strong biofilm producers had a greater number of twitching cells at 4 hours. Weak biofilm producers, on the other hand, had less number of twitching cells (Supplemetaory video S1: https://doi.org/10.1080/08927014.2022.2054703). One of the weak biofilm producers (TP-10) had no twitching motility. The colony edge formation of strong and weak biofilm producers

was also observed under phase-contrast microscopy. After 24 hours, a wrinkly colony edge was observed as a result of the higher number of twitching cells in strong biofilm producers (figure 4.5b, left panel). While, weak biofilm producers lacked fully wrinkled colony edge formation (figure 4.5b, right panel). T4P is made up of a single type IVa pilin protein expressed by the *pilA* gene in *P. aeruginosa*. The *pilA* gene expression levels were studied at 4 hours and 24 hours. At 4 hours, *pilA* gene expression of strong biofilm producers was 5-fold higher than weak biofilm producers (figure 4.5d) and 3-fold higher at 24 hours (Figure 4.5d).

4.3.6 CLSM of biofilm

Arrangements of live and dead cells within biofilm formed on the coverslip by strong and weak biofilm producers were observed by CLSM using syto9 and PI dyes. The orthogonal plane gives a more detailed idea of the arrangements of live and dead cells with the biofilm (Figures 4.6a and c). It can be observed through the orthogonal plane that strong biofilm producers have a smaller number of live cells and the greater number of dead cells (Figure 4.6 a). Whereas, a higher number of live cells was observed in biofilm formed by weak biofilm producers excluding TP-11 isolate biofilm where the cell death was more (Figure 4.4c). This could be due to increased pyocyanin production (in TP-11), as pyocyanin has been linked to cell death in *P. aeruginosa* (Das and Manefield 2012). Furthermore, the variation around the biofilm thickness of strong (31.25 µm ± 14.3) and weak (19.05 µm ± 9) biofilm producers were observed (Figures 4.6a and c). Closely packed cells were observed in biofilm formed by strong biofilm producers (Figure 4.6b), whereas loosely distributed cells were noted throughout the substratum in biofilm formed by weak biofilm producers of tiled images (Figure 4.6d). Further video of biofilm formed by strong and weak biofilm producers gives more detail about the arrangement of live and dead cells within the biofilm (Supplementary video S2: https://doi.org/10.1080/08927014.2022.2054703). In strong biofilm producers, the dead were densely packed within the biofilm substratum, whereas live cells were sparse and above dead cells. On other hand, biofilm formed by weak biofilm producers has a high number of live cells near the substratum than dead cells. Furthermore, from each Z stack of strong (n=4) and weak (n=4) biofilm producers, the number of live and dead cells was assessed. There was a significant difference in cell count (total cells and dead cells) within the biofilm of strong (n=4) and weak (n=4) biofilm producers (Figure 4.6c).

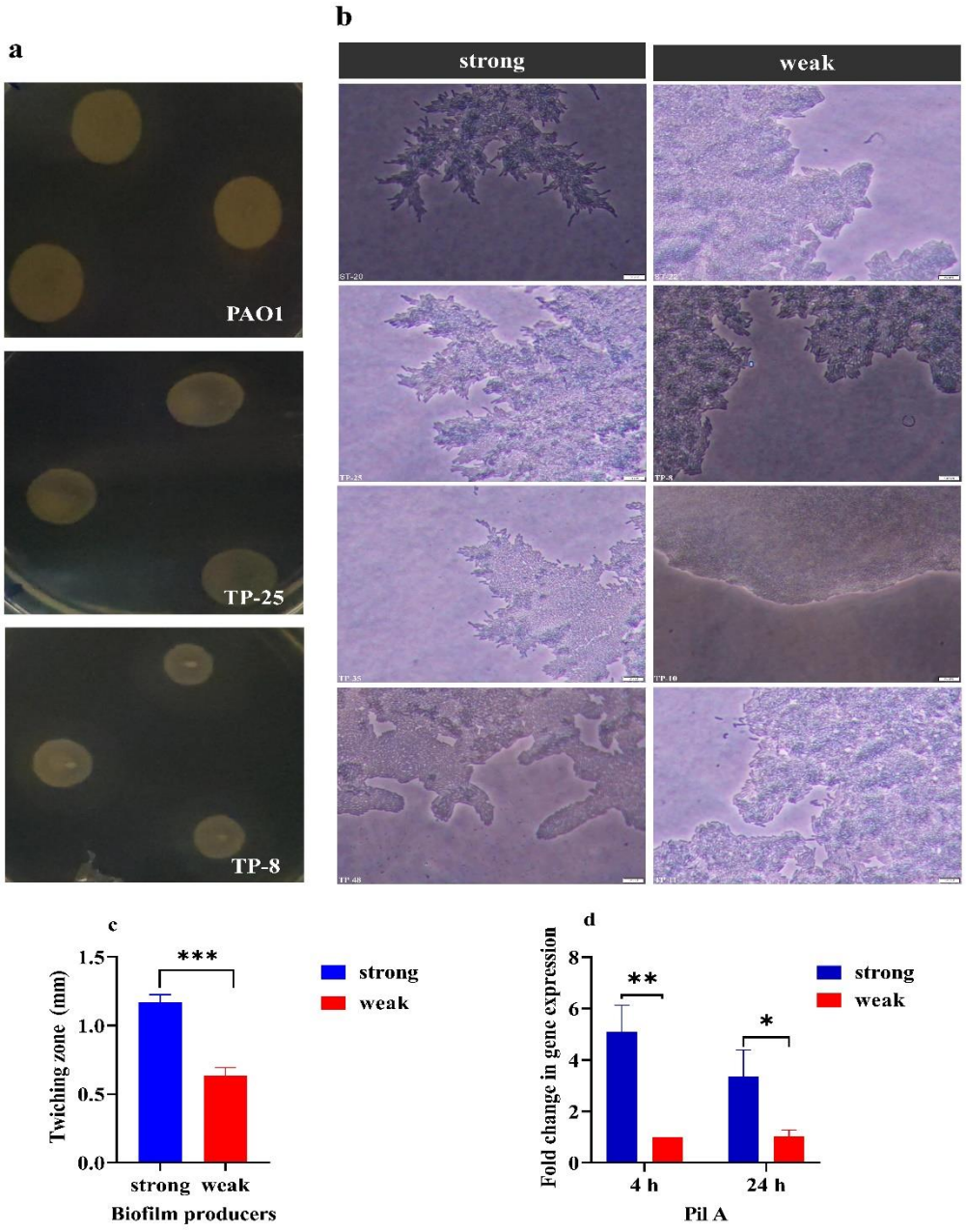

Figure 4.5: Twitching motility. (a) Representative twitching motility of PAO1, TP-25 (strong), and TP-8 (weak) on 1% LA. (b) Twitching zone of strong and weak biofilm producers. (c) Twitching motility was studied under Phase-contrast microscopy on a 1% LA pad. Representative Phase-Contrast Microscopy images of strong (n=4) and weak (n=4) biofilm producers. (d) The gene expression of *pilA* was studied at 4 hours and 24 hours. The data represent three biological triplicates for each strain. The statistically significant represents Student's t-test were * $P < 0.5$, ** $P < 0.05$, *** $P < 0.005$.

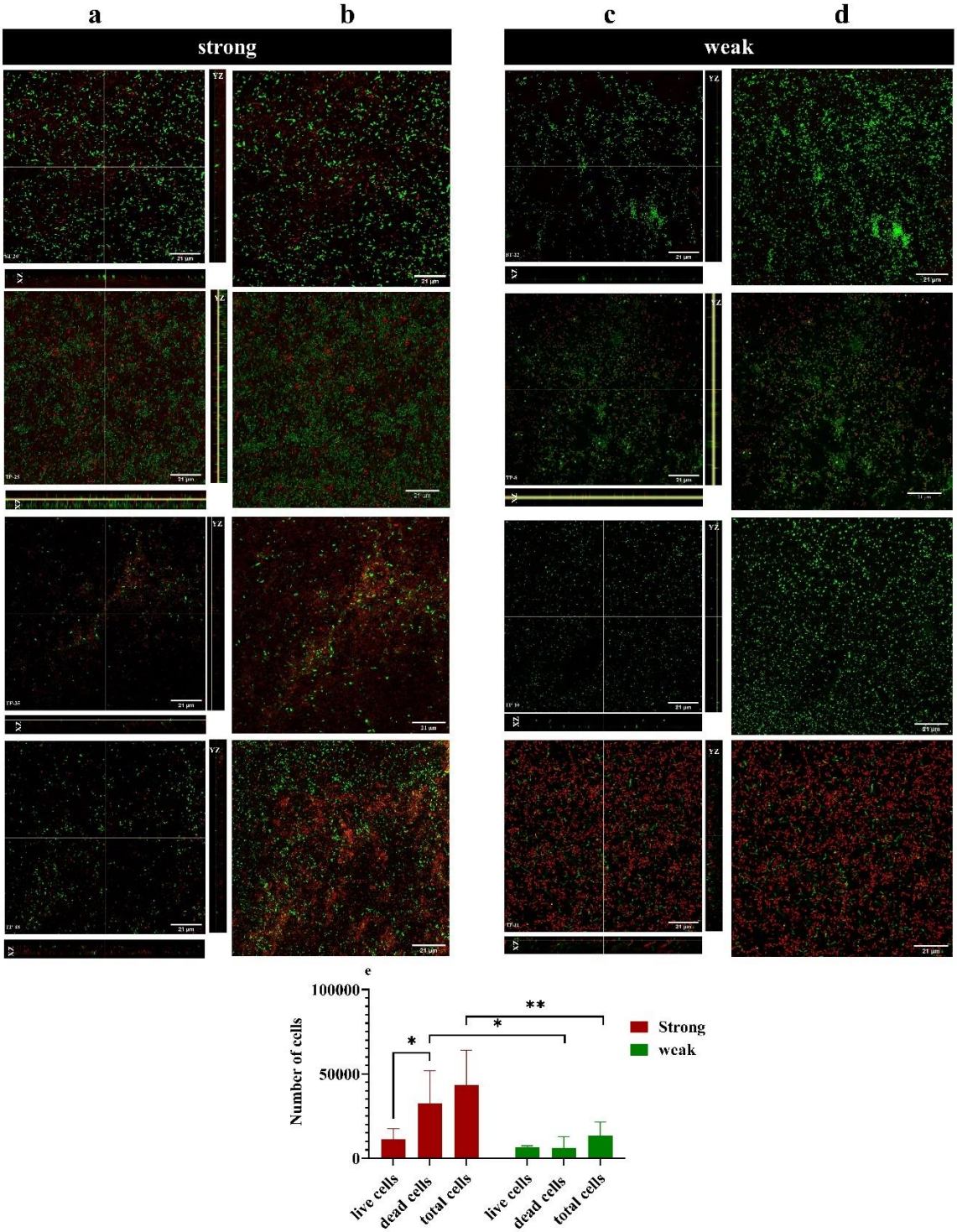

Figure 4.6: CLSM of biofilm formed by strong and weak biofilm producers. (a-d) The biofilm was formed on a coverslip for 24 hours which was visualized through CLSM using Syto 9 and PI dyes. The representative images of orthogonal view of (a) strong and (c) weak biofilm producers. The maximum intensity of biofilm is formed by (b) strong and (d) weak biofilm producers. The cell count of live, dead, and total cells (live and dead cells) within the Z-stack of strong and weak biofilm producers. The data

represent the mean and standard deviation. The statistical significance was performed using One-way ANOVA using GraphPad Prism 9, where ns $P > 0.05$, * $P < 0.05$, ** $P < 0.005$.

4.3.7 Components of biofilm

Biofilm components such as eDNA, an extracellular protein, pyocyanin, rhamnolipid, pel, and alginate exopolysaccharide were assessed among strong (n=4) and weak (n=4) biofilm producers. The amount of eDNA in strong biofilm producers (265 ± 130 µg/OD600) was significantly high compared to weak biofilm producers (44.96 ± 11.45 µg/OD600) (Figure 4.7a). Strong biofilm producers (17.45 ± 5.30 g/OD600) produced substantially more extracellular protein than weak biofilm producers (3.04 ± 1.20 g/OD600) (Figure 4.7b). Strong biofilm producers (120.10 ± 26.79 g/OD600) had considerably greater pel exopolysaccharide concentrations than weak biofilm producers (52.83 ± 23.38 g/OD600) (Figure 4.7c). However, in the case of alginate exopolysaccharide, pyocyanin, and rhamnolipid, there was no significant difference observed between strong and weak biofilm producers (Figure 4.7c and d). Further, no difference in *cdrA* gene expression was observed for strong and weak biofilm producers (Appendix 1).

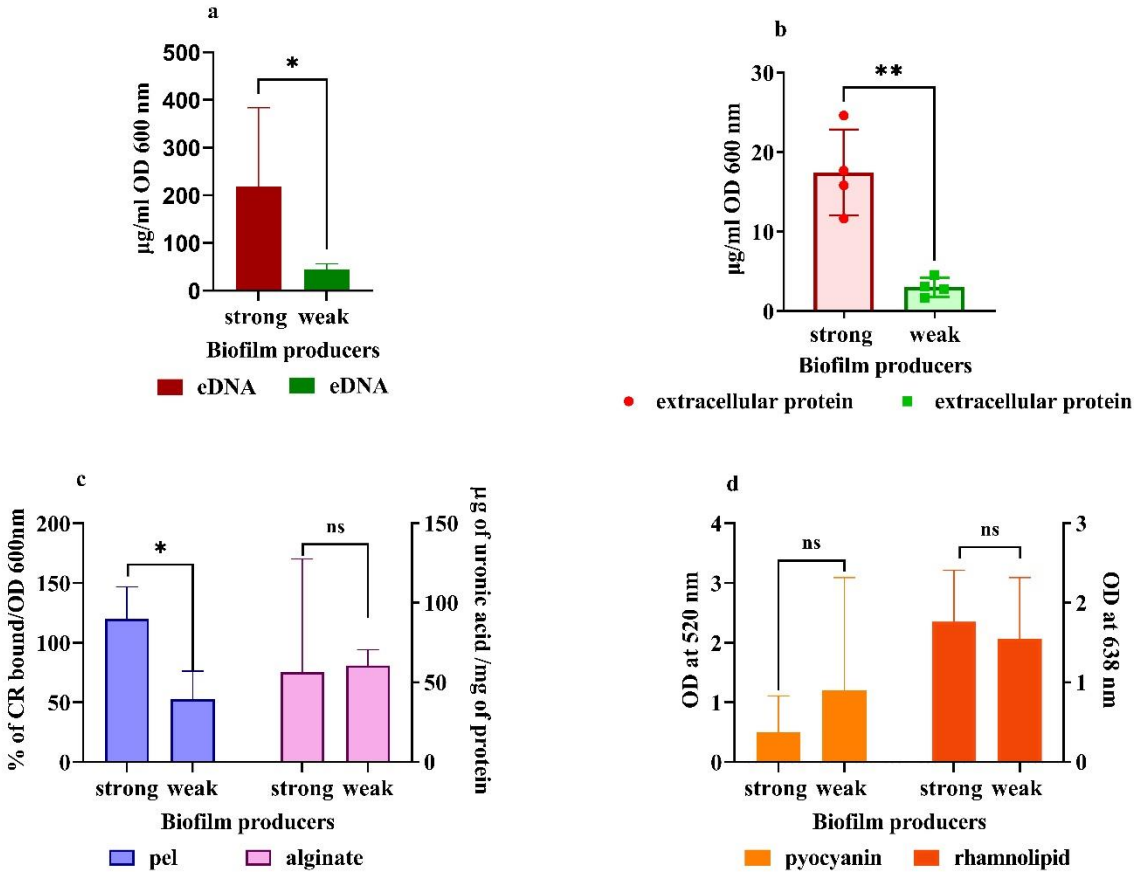

Figure 4.7: Quantification of biofilm matrix components. Quantification of (a) eDNA, (b) extracellular protein, (c) exopolysaccharide (pel and alginate), (d) pyocyanin and rhamnolipid in strong and weak biofilm producers. The error bar represents the mean and standard deviation. The statistical significance represents the student t-test using GraphPad Prism 9, where ns $P > 0.05$, * $P < 0.05$, ** $P < 0.005$.

4.3.8 Effect of exogenous treatments (enzymes, eDNA, proteins) on biofilm formation

The effect of different enzymes such as DNase I, proteinase K, and RNase was checked on biofilm formed by strong and weak biofilm producers. Within enzymes, proteinase K showed the highest inhibition of biofilm formed by strong biofilm producers, followed by RNase and DNase treatment, which decreased the biofilm by 76.35%, 63.43%, and 43.35 %, respectively (Figure 4.8a). whereas in weak biofilm producers only DNase treatment showed the reduction of biofilm by 58.27% (Figure 4.8a). We also speculated that adding exogenous DNA and extracellular protein might enhance the amount of biofilm. Although, a decrease in biofilm formation was observed in both strong and weak biofilm producers compared to the control (no eDNA is added) (Figure 4.8b). In addition, in comparison to the control, there was no significant difference in biofilm formation when extracellular protein was added (Figure 4.8c).

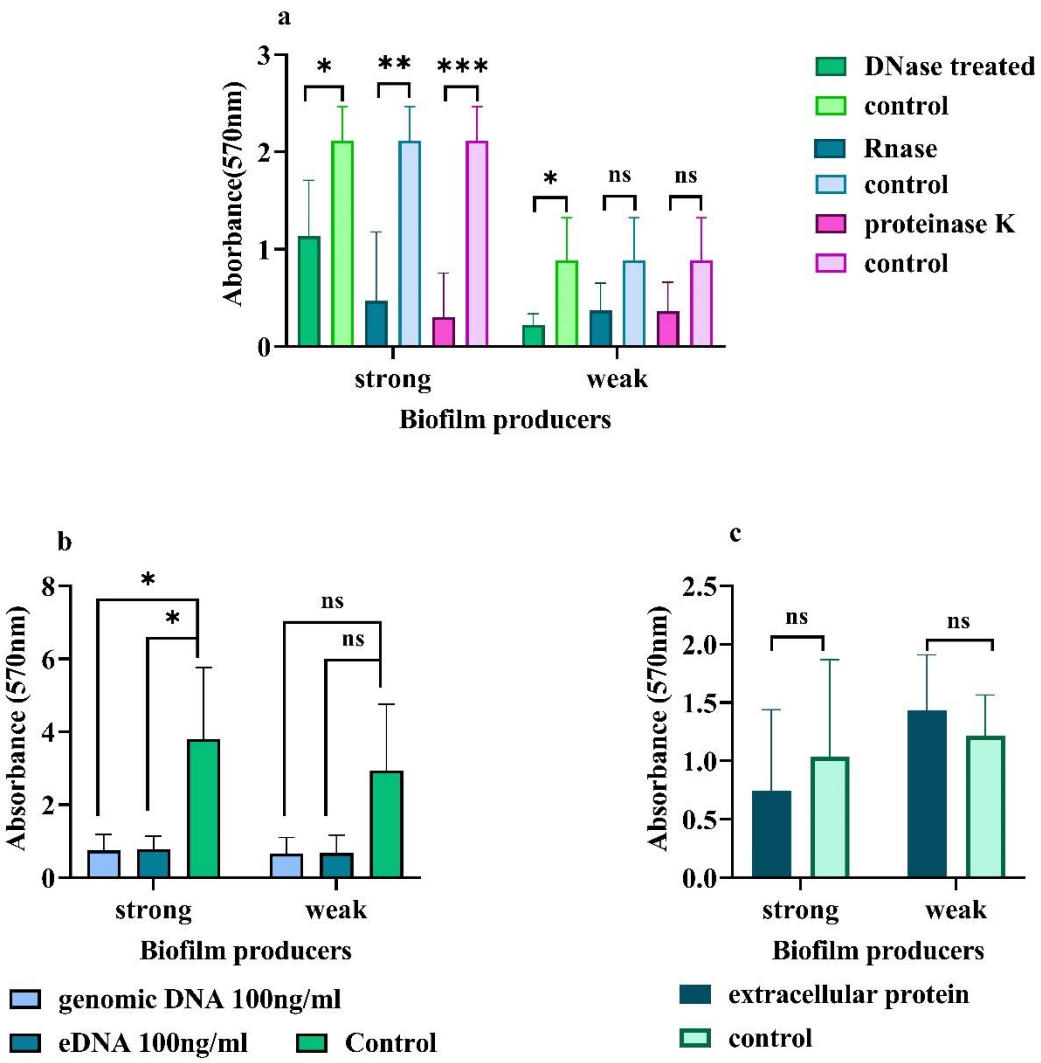

Figure 4.8: Effect of exogenous treatment on biofilm formation. (a) Effect of addition of DNase, RNase, and proteinase K on 24 hours biofilm (b) Effect of addition of genomic DNA (100 ng/ml) and eDNA (100 ng/ml) on biofilm, and (c) Effect of addition of extracellular protein on biofilm formation by strong and weak biofilm producers. The data represents mean ± stand deviation. Where the statistical significance was done using student t-test were ns $P > 0.05$, * $P < 0.05$, ** $P < 0.005$, *** $P < 0.0005$

4.4 Discussion

The well-known biofilm-forming bacteria *P. aeruginosa*, effectively colonizes different surfaces (biotic or abiotic), causing chronic infections such as cystic fibrosis, UTIs and that are difficult to eradicate (Brindhadevi et al. 2020). There is little information regarding the biofilm formation related to UTIs causing *P. aeruginosa*. Finding out whether the UTI isolates of *P. aeruginosa* differed in their ability to form biofilms was the first objective of this study, where the majority of the isolates were strong biofilm producers. No variation in biofilm formation on catheters (silicone-coated latex and silicone) was observed, apart from this, all isolates produced biofilm on catheters in the following order: LB > NU > AU medium. The formation of biofilm is greatly influenced by material properties. Here the silicone-coated latex catheter used in this study is the most commonly used material among urinary catheters because of its durability and flexibility (Vipin et al. 2019). One recent study showed that weak biofilm producers form strong biofilm on silicone-silicone-coated latex catheters in tryptone soya broth (Vipin et al. 2019). This might be due to high adhesion on the porous surface of silicone-coated latex catheters which facilitates the formation (Lee et al. 2017), whereas silicone catheters are known to have a smooth surface and decrease cell adhesion (Feneley et al. 2015). The different surface influences biofilm formation, where one study showed a 96-well polystyrene plate with a hydrophobic surface and a glass surface that has noticeably high biofilm formed by *P. aeruginosa* in presence of LB medium (Asghari et al. 2021). Apart part from these cole et al 2018 reported that urea present in urine, a host factor inhibits the gene expression of quorum sensing (pyocyanin production and rhamnolipid production) of *P. aeruginosa* (Cole et al. 2018). As a result, in this study, there was a decrease in biofilm formation in presence of NU and AU compared to LB (Figure 4.2). Many variables such as surface properties, cell surface hydrophobicity, medium and cell appendages (flagella and T4P) (Zheng et al. 2021) might contribute to the diverse behavior of clinical isolates. Where one study reported that 54% of *P. aeruginosa* from keratitis showed biofilm formation (Heidari et al. 2018) Sayran Hamad Haji 2018. Further, major studies have focused on antibiotic resistance from UTIs causing P. aeruginosa (Saxena et al. 2014; Karballaei Mirzahosseini et al. 2020; Kamali et al. 2021) and there is little information regarding the biofilm formation quantification by clinical isolates of *P. aeruginosa* causing UTIs.

A limitation of the present study is that the initial categorization of strong, moderate, and weak biofilm producers were done using CV assay in the 96-well polystyrene plates. As CV stains all the biofilm components (live-dead cells, proteins, RNA, eDNA, polysaccharides, etc.),

therefore it was used as the initial indicator. Later, to find the differences between biofilms formed by strong and weak biofilm producers other techniques like microscopy (light, CLSM, and SEM microscopy) and biochemical assays were used. Therefore, a glass coverslip was used for adhesion assays and CLSM, whereas, catheters (silicone-coated latex) were used for SEM. The variation in biofilm formation in strong and weak biofilm producers might be due to differences in twitching motility, adhesion, and components of the biofilm matrix. In this study, the cell adhesion (Figure 4.4), twitching motility (Figure 4.5 a-c), and expression of the *pilA* gene (Figure 4.5d) were high in strong biofilm producers. The T4P are well-known cell-associated virulence factors located at the pole of the cell and required for biofilm formation expansion through twitching motility through rounds of extension, surface attachment, and retraction (Comolli et al. 1999; Burrows 2012). Twitching motility promotes active biofilm expansion across the indwelling catheters in *P. aeruginosa* (Rodney M. Donlan 2001; Sabbuba et al. 2002; Stickler 2008). In the study on clinical and environmental isolates, the motility phenotype was present, and an increase in biofilm formation was observed (Head and Yu 2004; Inclan et al. 2011). A recent study on 190 clinical isolates of *P. aeruginosa* found that twitching motility was more in high biofilm formation isolates, whereas isolates having high swimming and swarming motility failed to produce a strong biofilm (Horna et al. 2019). The T4P is responsible for biofilm formation and twitching motility-mediated active biofilm expansion through rounds of extension, surface attachment, and retraction (Whitchurch 2006; Gloag et al. 2013). A multitude of complicated regulatory systems, including a putative chemosensory system called the Chp system, control the biogenesis, assembly, and twitching motility function of T4P (Whitchurch 2006) and various other complex systems control the T4P responses. As a result, it is difficult to understand the behavior of T4P in response to various signals. The gene cluster pilGHIJK-chpABC encodes for the T4P system (Darzins 1993; Darzins 1994; Darzins 1995; Whitchurch et al. 2005). Cellular levels of either c-di-GMP or cAMP, which are the two main factors influencing the motility-sessility switch in *P. aeruginosa*, have both been reported to rise during growth on solid media (Hengge 2009; Römling et al. 2013; Valentini and Filloux 2016). In response to external signals, the levels of c-di-GMP and cAMP are modified by several sensing systems, which include the chemotactic cluster (PilGHIJK -ChpABC) and chemosensory clusters (WspA, WspR, Gac-Rsm, and RocS1), respectively. Previous studies have shown *P. aeruginosa* twitching motility in response to serum albumin (in the form of BSA), mucin, and oligopeptides (in the form of tryptone) and shown that FimX is involved in the response to substances (Huang et al. 2003). Further, *P. aeruginosa* can come across host signals such as oligopeptides (present in urine), and serum albumin (vicinity of epithelium

cells) via twitching motility which helps in the colonization of implant devices, CF lungs, and epithelial cells. In presence of tryptone, BSA, and mucin the levels of T4P and cAMP were elevated through ChpC of the Chp chemosensory system (Nolan et al. 2020). The same study found that protease activity is necessary for twitching movement, likely to release smaller albumin, mucin, and tryptone, such as Gln, and di- or oligo-peptides. These smaller components can then be sensed either directly by methyl-accepting chemotaxis proteins (MCP) that feed into the Chp system via ChpC or indirectly by one or more of the 98 solute-binding proteins (SBPs) in *P. aeruginosa* (Darzins 1994; Nolan et al. 2020). In addition, it was hypothesized that the twitching motility is modulated by environmental signals sensed through SBPs associated with MCP/pilJ, which is further associated with chpA by Pill/ChpC/CheW. Further, biofilm is reported to be formed independent of exopolysaccharide (pel. Psl and alginate) via eDNA release by urea through unknown mechanism (Cole et al. 2014). The eDNA present in *P. aeruginosa* biofilms has also been shown to regulate twitching motility via co-ordinating bacterial movements at leading edge rafts during biofilm expansion (Gloag et al. 2013). Further, Schaik et al 2005 demonstrated that T4P can bind directly to any form of DNA prefertianlly to pyrimidine bases (Schaik et al. 2005). The ability of T4P to bind to DNA may play role in biofilm formation during infection or colonization on abiotic surface. Apart from this it also act as nutrient source during starvation and determine antibiotic resistance (Allesen-Holm et al. 2006). Overall, a vast range of environmental and host signals have been shown to stimulate twitching and these signals along with the genomic diversity of clinical isolates lead to differences in biofilm formation among clinical isolates of *P. aeruginosa*.

Further, an increase in eDNA, an extracellular protein, and pel polysaccharide in biofilms formed by strong biofilm producers was observed (Figure 4.7a,b and c). The *in vivo* studies from chronically infected CF patients' tissue have found the eDNA surrounding biofilm (Alhede et al. 2020). The *in vitro* studies have highlighted the eDNA presence in the inner part of biofilm, while *in vivo* biofilm, eDNA is concentrated in the outer layer of the biofilm (Whitchurch et al. 2002; Ciszek-Lenda et al. 2019; Alhede et al. 2020). Recent studies have shown the eDNA in fragment form in the hyper biofilm producer formed by rugose small colony variant (RSCV) a *P. aeruginosa* strain variant which enables the more resistant structure (Deng et al. 2020). Over the past few years have focused on eDNA (one of the components of *P. aeruginosa* biofilm) as it is responsible for bacterial tolerance and infection (Mulcahy et al. 2010; Chiang et al. 2013; Ciofu and Tolker-Nielsen 2019). One mechanism of eDNA release is the cell death of *P. aeruginosa* within the biofilm and similar to programmed cell death in

eukaryotes. There are several mechanisms of cell death and eDNA release in the environment of *P. aeruginosa* of which one such mechanism is lambda prophage induction (Webb et al. 2003). Another mechanism reported is through quorum sensing molecules (AHL and PQS) which increase the ROS production or pyocyanin production causing damage to the cell membrane and which leads to cell autolysis (Webb et al. 2003; Allesen-Holm et al. 2006; Hazan et al. 2016; Tahrioui et al. 2019). Pyocyanin is a well-known virulence factor and secondary metabolite. Das and Manefield demonstrated that eDNA is also released in *P. aeruginosa* biofilm through pyocyanin production resulting in H_2O_2 production due to which cell death occurs (Das and Manefield 2012). 4-hydroxy-2-heptylquinoline N-oxide (HQNO), an inhibitor of cytochrome is responsible to release eDNA via the production of reactive oxygen species (ROS) in cells causing membrane damage resulting in cell autolysis (Déziel et al. 2004; Hazan et al. 2016). The hydroxy-2-alkylquinolines and PrrF small regulatory RNAs play important role in the shaping of the biofilm. All above eDNA release mechanisms is recently reviewed in detail by Sakar (Sarkar 2020). In a biofilm, eDNA is released into the biofilm matrix through cell autolysis (Webb et al. 2003). Apart from this, Pel is a cationic exopolysaccharide cross-linked with extracellular DNA to provide stability and structural integrity to the *P. aeruginosa* biofilm (Jennings et al. 2015). The numerous mechanisms mentioned above could contribute to cell death and eDNA release in the biofilms. Therefore, additional studies using the clinical isolates are necessary to determine whether the aforementioned pathways are potentially involved in cell death. Increased cell death in TP-11(weak biofilm producer) biofilm may be caused by pyocyanin production (Figure 4.6 c and d). Apart from cell death, other factors could contribute to strong biofilm formation. In addition to eDNA, the *P. aeruginosa* biofilm matrix also includes proteins with protective, structural, and other functional roles (Borlee et al. 2010; Tseng et al. 2018). The first biofilm matrix protein CdrA was reported in *P. aeruginosa* which contributes to the structural integrity of biofilm Borlee BR 2010. Through interaction with CdrA-Psl (Borlee et al. 2010) CdrA-Pel (Reichhardt et al. 2020) and CdrA-CdrA interactions (Reichhardt et al. 2018), CdrA enhances biofilm stability and aggregation. These interactions, corresponding, help biofilm to resist mechanical disruption and proteolytic degradation in the host environment (Reichhardt et al. 2018). The presence of CdrA protein in clinical strains isolated from CF patients was varying (Borlee et al. 2010). However, in the present study, there is no difference in *cdrA* gene expression of strong and weak biofilm producers (Appendix 1). Further, a recent study conducted showed that 60 matrix-associated proteins were found using a non-invasive proteomic approach. The same

study also reported that biofilm-matrix protein ecotin (PA2755) levels were high during the biofilm development and associated with biofilm exopolysaccharide Psl (Tseng et al. 2018). Apart from this, ecotin protein shields the planktonic as well as biofilm cells from neutrophil elastase killing. Also, a study evaluating matrix-associated proteins recovered from several phases of *P. aeruginosa* ATCC27853 biofilms using iTRAQ-based quantitative proteomics revealed that 54 distinct proteins changed intermittently during biofilm formation (Zhang et al. 2015). It can be hypothesized that *P. aeruginosa* biofilm-matrix proteins are highly dynamic during different biofilm phases and many proteins are involved. Future studies on extracellular proteins in biofilm matrix are needed on clinical isolates of UTIs.

Cole *et al* 2014 attributed that *P. aeruginosa* stains having *pel* and *psl* genes form robust biofilm *in-vitro* and during CAUTIs in the murine model than deficient strains (Cole et al. 2014). In the early phases of biofilm development, the exopolysaccharide Psl is attached to the cell surface and acts as an adhesin, later on, it relocates as a peripheral exopolysaccharide (Ma et al. 2009). Here Psl exopolysaccharide was not measured is the limitation of this study. While another exopolysaccharide Pel was found high in strong biofilm producers. The Pel exopolysaccharide can serve as a structural and protective factor in biofilm, also it can compensate for T4P/other adhesins as an attachment factor during biofilm development (Vasseur et al. 2005; Colvin et al. 2011). Rhamnolipids are found in *P. aeruginosa* biofilms which plays important role in maintaining biofilm structure as well as the dispersion of sessile cells from biofilm. (Davey et al. 2003; Boles et al. 2005; Pamp and Tolker-Nielsen 2007). However, in the present study, no difference was observed in *P. aeruginosa* biofilm.

Biofilm becomes more susceptible to antibiotics after DNase treatment as eDNA is removed (Tetz et al. 2009; Kaplan et al. 2012). Here in this study biofilm was strongly inhibited in strong and weak biofilm producers (Figure 4.8a). However, with the addition of genomic DNA and eDNA no increase in biofilm was observed in strong and weak biofilm producers (Figure 4.8b). This might be due to the addition of an excess amount of eDNA inhibited growth of planktonic bacteria as well as biofilm formation (Mulcahy et al. 2008). Further, Deng 2020 reported the addition of digested genomic DNA increased biofilm formation through DNA-protein interaction (Deng et al. 2020). In *Haemophilus influenza*, nucleoid-associated proteins are connected to eDNA strands (Goodman et al. 2011). Further Proteinase K treatment decreased in biofilm formation was observed compared to no treatment (Reichhardt et al. 2018).

Disruption of eDNA-protein interaction results in the dispersion of *Burkholderia cenocepacia* biofilms (Novotny et al. 2013).

From the above results, high adhesion ability and twitching motility contribute to strong biofilm formation. There is variation in weak biofilm-producing isolates. As biofilm-related infections are difficult to treat, twitching motility, eDNA, and high adhesion ability in the early stages of biofilm formation can be used as therapeutic targets for biofilm formation